Columnar Mesomorphism in Hexacatenar Tetrahedral (2,2′-Bipyridine)zinc Complexes and Homologous Palladium Derivatives

Giovanna Barberio,[a] Anna Bellusci,[a] Alessandra Crispini,[a] Mauro Ghedini,[a] Attilio Golemme,[a] Piotr Prus,[a] and Daniela Pucci*[a]

Keywords: Bipyridine ligands / Zinc / Palladium / Metallomesogens / Columnar structures

The synthesis and characterisation of novel liquid crystals which display columnar mesomorphism induced upon complexation of a series of nonmesomorphic hexacatenar 4,4′-disubstituted 2,2′-bipyridines (**L^n**) are reported. The introduction of different metal centres (Zn, Pd) causes the appearance of mesomorphism in all complexes regardless of the geometry around the metal ion. We therefore report the first examples of mesomorphism in tetrahedral zinc derivatives. The nature of the columnar phases is related to the self-assembly of the half-disc shaped [**L^{n}MCl$_2$**] (M = Zn, Pd) complexes into full disc-shaped supramolecules. The molecular organisation in the mesophase is mainly driven by intermolecular attractive interactions, as shown by the crystal structure of the model compound [**LPdCl$_2$**]. Preliminary measurements of photoconductivity have been performed on samples of [**L^{n}MCl$_2$**] complexes doped with C_{60} to increase absorption. Promising results were obtained.

Introduction

The role of metal ions in the formation of molecular motifs and intermolecular interactions, which are unapproachable for organic liquid crystals and promote mesomorphism in nonmesogenic ligands, continues to make metallomesogens promising materials with novel and interesting properties.[1−6] In particular, the design of suitable metal-ligand combinations represents a challenge for obtaining new functional liquid crystalline materials by molecular self-assemblies.[7]

In this context, we recently reported[8] the synthesis of a series of nonmesomorphic dialkyl 2,2′-bipyridine-4,4′-dicarboxylates for which the complexation with various metal salts resulted in [(Bipy)MX$_2$] (M = Pd, Pt, Ni, Zn) species which self-assemble in dimers built up from attractive intermolecular interactions. This is described by the complementary shape approach.[9]

Due to the overall shape of the stacked units, these complexes exhibit lamellar mesomorphism which depends mostly on the geometry of the metal centre. In fact, the zinc homologues do not exhibit liquid crystalline properties due to their tetrahedral coordination. In continuation of our previous studies on the relationship between molecular structures, symmetry prerequisites and mesomorphism, we have been interested in the design of a further class of 4,4′-disubstituted 2,2′-bipyridines in order to induce, upon complexation, a molecular disc shape and columnar mesomorphism in the corresponding supramolecular metal aggregates. Moreover, since discotic liquid crystal systems have recently gained interest because of new applications in molecular electronics and optoelectronics,[10−12] we wanted to investigate if the design of supramolecular disc-like metallomesogens, with a long-range molecular order, would be advantageous for the enhancement of pre-selected properties such as charge transport or luminescence. The attractiveness of these systems is also demonstrated by the fact that during the preparation of the current article an apparently similar study was reported.[13] However, although the same methodology was used for inducing columnar mesophases in hemi-disc like complexes, Donnio et al. carried out their studies on terdentate ligands such as the 2,6-bis[3′,4′,5′-tri(alkoxy)phenyliminomethyl]pyridines and consequently the discrete building blocks show very different geometric features.

In the present work we report the synthesis of a series of hexacatenar 4,4′-disubstituted 2,2′-bipyridine ligands and related *cis*-dichloro zinc and palladium derivatives. The single-crystal X-ray structure of the palladium model complex [**LPdCl$_2$**] is also reported and discussed. The liquid crystalline properties of all [**L^{n}MCl$_2$**] (M = Zn, Pd) complexes which, in contrast to the free ligands, exhibit columnar mesomorphism are also described. It should be noted that rigid tetrahedral molecules usually seem to prevent mesophase formation[14] and the only examples of mesomorphic zinc derivatives to date exhibit either a trigonal-bipyramidal geometry with dithiobenzoate[1] or terpyridine

[a] LASCAMM, Unità INSTM della Calabria, Dipartimento di Chimica, Università della Calabria,
87030, Arcavacata (CS), Italy
Fax: (internat.) + 39-0984-492066
E-mail: d.pucci@unical.it

ligands[13,15] or a square-planar geometry when the metal centre is incorporated in a porphyrin or a phthalocyanine core.[1,16] Moreover, preliminary measurements of photoconductivity have been performed on samples of [$\mathbf{L^nMCl_2}$] doped with C_{60} to increase absorption. Promising results were obtained.

Results and Discussion

Synthesis and Characterisation

The hexacatenar $\mathbf{L^n}$ ligands (where n denotes the number of carbon atoms in the alkoxy chains) were prepared as white solids, in high yields, from the reaction of the 4,4′-bis(hydroxymethyl)-2,2′-bipyridine with the appropriate 3,4,5-trialkoxy-substituted benzoic acid using a DCC-PPY esterification (Scheme 1). The model ligand **L**, without the six alkoxy chains grafted on the peripherical phenyl rings, has been synthesised in an analogous manner by treating the 4,4′-bis(hydroxymethyl)-2,2′-bipyridine with benzoic acid.

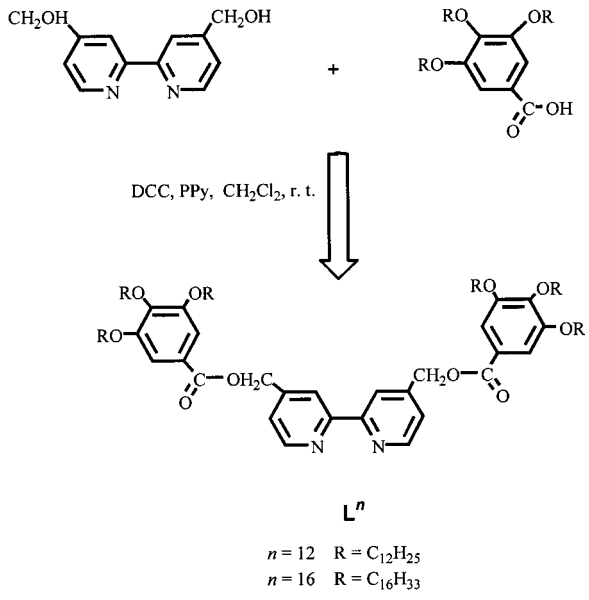

Scheme 1. Synthetic route to the hexacatenar $\mathbf{L^n}$ ligands

The hexacatenar complexes [$\mathbf{L^nMCl_2}$] as well as the model complexes [$\mathbf{LMCl_2}$], were prepared by treatment of an equimolar amount of the appropriate ligand with $ZnCl_2$ (in dichloromethane at room temperature) or $[Pd(PhCN)_2Cl_2]$ (in chloroform at reflux), respectively.

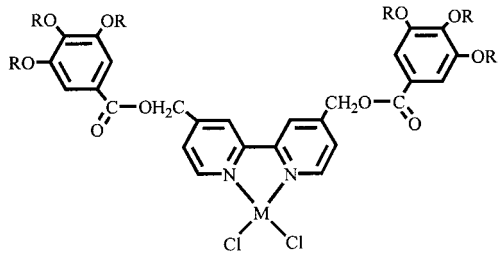

[$\mathbf{L^nMCl_2}$]
M = Zn, Pd

The structures and purities of all the ligands and complexes were confirmed by IR and ^{1}H NMR spectroscopy and elemental analyses. In the ^{1}H NMR spectra of these complexes the H3 and H6 bipyridinic proton resonances shifted (by about 0.3 ppm) up and down field with respect to their organic precursors. These observations confirmed the coordination of the bipyridines to the metal fragments.

Single-Crystal X-ray Diffraction of [$\mathbf{LPdCl_2}$]

The [$\mathbf{LPdCl_2}$] complex was synthesised and then structurally characterised with the explicit intention of giving more insight into the molecular organisation in the 3D space of these new (2,2′-bipyridine)metal complexes in which the 4,4′-disubstituents are now different from the carboxylates with long alkyl chains already discussed in a previous paper.[8b] Moreover, in the absence of diffraction-quality crystals for any of the long-chain homologues, [$\mathbf{LPdCl_2}$] could be considered as a model compound and its molecular organisation taken as being representative for the discussion of the liquid-crystalline states of similar mesogenic complexes. The structure of [$\mathbf{LPdCl_2}$] is shown in Figure 1 and a selection of bond lengths and angles is reported in Table 1.

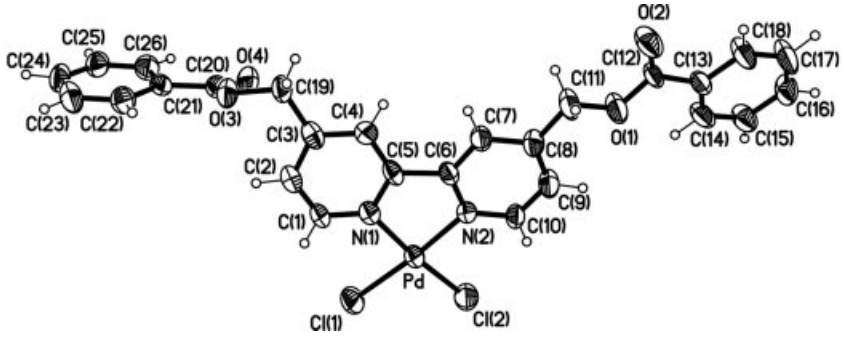

Figure 1. Molecular structure and atomic labelling scheme (50% probability thermal ellipsoids) of complex [$\mathbf{LPdCl_2}$]

Table 1. Selected bond lengths (Å) and angles (°) for complex **[LPdCl$_2$]**

Pd−N(1)	2.023(5)	Pd−N(2)	2.034(4)
Pd−Cl(1)	2.283(2)	Pd−Cl(2)	2.283(2)
N(1)−Pd−N(2)	80.9(2)	Cl(1)−Pd−Cl(2)	90.0(7)
N(1)−Pd−Cl(1)	94.0(1)	N(1)−Pd−Cl(2)	174.4(1)
N(2)−Pd−Cl(1)	174.9(2)	N(2)−Pd−Cl(2)	95.0(1)

The palladium atom has a distorted square-planar geometry and the bond lengths and angles around the metal ion and within the five-membered chelate ring are similar to those recently reported by us for the complex (dihexadecyl 2,2′-bipyridyl-4,4′-dicarboxylate)palladium(II) chloride.[8b] The two substituents on the 2,2′-bipyridine ligand run in opposite directions as shown by the dihedral angles C(4)−C(3)−C(19)−O(3) and C(7)−C(8)−C(11)−O(1) of 171.6(5) and −162.5(5)°, respectively. While the carboxylic oxygen atom O(2) points toward the internal part of the bipyridine ligand [C(12)−O(1)−C(11)−C(8) 180.0(5)°], O(4) shows a very different orientation [C(20)−O(3)−C(19)−C(3) −76.2(6)°]. The asymmetry in the conformation around the "CH_2−O" bond of the two substituents can be clarified by considering the crystal packing of molecules of the **[LPdCl$_2$]** complex.

The molecular organisation is dominated by intermolecular interactions of two main types: i) hydrogen bonds (C−H···O and "aromatic hydrogen bonds" C−H···π[17]) and ii) π−π contacts (Figure 2 a).

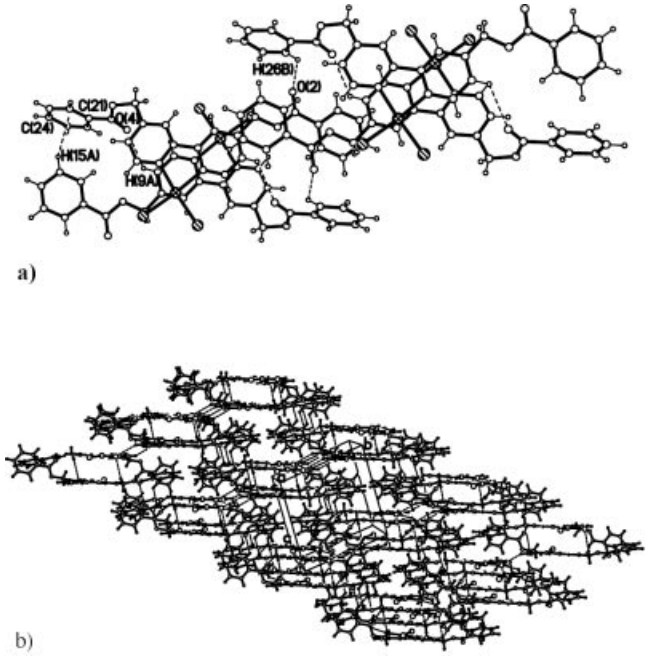

Figure 2. Ball and stick representation of interacting dimers of **[LPdCl$_2$]** viewed approximately down the *c* axis (top view) and repetition of dimers in 3D space with generation of a columnar arrangement (bottom view)

The association of molecules into dimers (superimposed approximately along the c axis) related by an inversion centre is characterised by the presence of hydrogen bonds between the carboxylic oxygen atoms and one of the pyridine hydrogen atoms [C(9a)···O(4) = 3.17(1) Å, H(9a)···O(4) 2.54(1) Å, C(9a)−H(9a)···O(4) 124.8(5)°, a = $-x$, $-y$, $-z$]. The reciprocal orientation of the C(21)/C(26) phenyl ring with respect to the centrosymmetric C(13)/C(18) ring with a dihedral angle of 66° is able to create an interesting intermolecular contact of the C−H/Ph type, for which the distance between H(15a) and the aromatic centroid X of the C(21)/C(26) ring (2.68 Å) and the C(15a)−H(15a)···X angle (147°) are indicative of the presence of a weak hydrogen C−H-π bond.[17] Moreover, the disposition of the pyridinic aromatic rings gives rise to a parallel displaced π−π stacking arrangement characterised by a centroid contact of 3.52 Å, an angle of 18° between the ring normal and the centroid vector and a corresponding horizontal displacement of 1.20 Å.[18] The M···M intermolecular separation of 5.6 Å within the dimer is significantly different from any weak Pd···Pd attractive interaction. The carboxylic oxygen atom O(2) which is not involved in any significant interaction within the dimer, assists in holding dimers together through the formation of hydrogen bonds with one of the hydrogen atoms of the peripheral phenyl rings (see a in Figure 2). In 3D space, the repetition of dimers which are stacked along the c direction and separated by layers of interacting aromatic rings (see b in Figure 2) is of particular interest in the discussion of the columnar organisation found for the analogous complexes **[L^{n}MCl$_2$]** with long alkoxy chains on the peripheral aromatic rings in the liquid crystalline state. Moreover, the absence of solvent molecules in the crystal packing enables us to view this molecular arrangement as a fingerprint for identification of future columnar liquid crystalline organisations.

Thermal Behaviour of [L^{n}MCl$_2$] Complexes

Although hexacatenar 2,2′-bipyridine ligands are not liquid crystals, all **[L^{n}MCl$_2$]** complexes show enantiotropic columnar mesomorphism which was investigated using polarised optical microscopy (POM), differential scanning calorimetry (DSC) and temperature dependent powder X-ray diffraction (PXRD) measurements. The thermal data of the **[L^{n}MCl$_2$]** series are summarised in Table 2.

For all **[L^{n}MCl$_2$]** complexes the results from POM suggested the presence of a columnar hexagonal mesophase, as indicated by the typical pseudo-focal-conics and areas of homeotropic orientation (Figure 3).

The dodecyloxy homologues feature two mesophases as shown by DSC and confirmed by subtle textural changes, such as the appearance in POM of fine disclination lines and deeper colours at the second order transition. This could indicate a transition between two hexagonal phases with different degrees of order within the columns. In the case of the palladium complexes, cooling from the isotropic liquid did not lead to crystallization but instead to solidification into a glassy state retaining the structure of the hexagonal mesophase.

Table 2. Optical and thermal data of [L^nMCl_2] complexes

Compound	Transition[a]	T/°C[b]	ΔH/kJ·mol^{-1}
	Cr − Col_{h1}	46.2	24.5
	Col_{h1} − Col_{h2}	122.6	15.0
[$L^{12}ZnCl_2$]	Col_{h2} − I	132.1	2.7
	I − Col_{h2}	131.0	2.1
	Col_{h2} − Col_{h1}	110.6	15.2
	Col_{h1} − Cr	56.7	30.0
	Cr − Cr′	58.5	73.7
	Cr′ − Col_h	90.6	37.7
[$L^{16}ZnCl_2$]	Col_h − I	111.4	8.0
	I − Col_h	111.1	1.3
	Col_{h1} − Cr′	59.3	24.7
	Cr − Col_{h1} [c]	76.0	102.5
[$L^{12}PdCl_2$]	Col_{h1} − Col_{h2}	136.4	30.0
	Col_{h2} − I	145.3	1.26
	I − Col_{h2}	145.2	2.5
	Cr − Col_h	48.6	20.8
[$L^{16}PdCl_2$]	Col_h − I	127.5	20.9
	I − Col_h	112.5	9.4

[a] Cr: crystal; Col_h: columnar hexagonal; I: isotropic liquid. [b] Temperature data as peak onset.[c] Microscopy data.

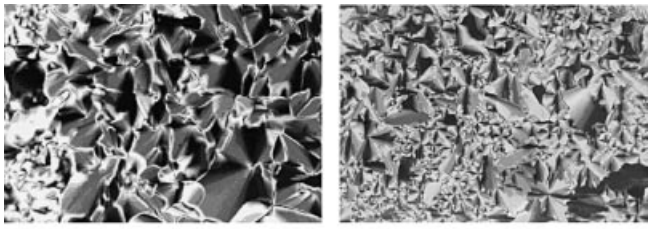

Plate 1 *Plate 2*

Figure 3. Polarised light optical photomicrograph of the texture exhibited by [L^nMCl_2] complexes; plate 1: texture of the hexagonal columnar mesophase of [$L^{12}ZnCl_2$] at 128 °C; plate 2: texture of the hexagonal columnar mesophase Col_{hd1} of [$L^{12}PdCl_2$] at 135 °C

The mesophases were also identified by temperature-dependent powder-XRD experiments. The X-ray diffraction patterns confirmed the results of optical microscopy. In all cases, in the small angle region a sharp high intensity peak and two lower intensity peaks at wider angles were indexed to the (1 0), (1 1) and (2 0) reflections. This is typical of a 2D hexagonal lattice (Table 3).

Moreover, in the case of [L^nMCl_2], a transition between hexagonal phases was observed. As shown in Figure 4 for [$L^{12}ZnCl_2$], in the wide angle region of the XRD spectrum recorded at 90 °C, the pattern consists of a broad diffuse scattering halo (B in Figure 4) at ca. 4.6 Å, corresponding to the liquid-like disorder of the aliphatic chains. Also observed was another broad diffuse band (C in Figure 4) at ca. 4.1 Å which is characteristic of the distance between adjacent cores (also definable as the stacking period in a column)[19] and, finally, a third less intense broad band (A in Figure 4) at ca. 8 Å possibly indicating a perpendicular stacking of the hemi-disc shaped molecules which is necessary to produce a disc-shaped dimer for the formation of the columnar phase.[20]

The proposed model of organisation in the hexagonal phase is in accordance with the calculated number of molecules in the cross section of the columns. This value, which was found to be around 2, was estimated by assuming a density of 1 g·cm^{-3} and a height for the columnar slice of 4.1 or 4.7 Å for M = Zn and 3.8 or 4.6 Å for M = Pd (Table 3). The transition Col_{h1} − Col_{h2} is accompanied by a decrease in the hexagonal lattice constant and a loss of the broad diffuse band centred at 4.1 or 3.8 Å (Table 3). These differences may characterise Col_{h2} as a more disordered hexagonal phase than Col_{h1}. Within the temperature range in which the first hexagonal phase may be observed, the lattice parameter was found to be temperature dependent. In fact, the low angle reflection shifted to a larger d spacing with decreasing temperature indicating a lattice expansion.[21]

A further increase in the number of carbon atoms in the side chains was not accompanied by any change of sym-

Table 3. X-ray diffraction data of [[L^nMCl_2] complexes

Compound	Mesophase Lattice constants/Å	$d_{obsd.}$/Å (d_{calcd}/Å)	Miller indices
[$L^{12}ZnCl_2$]	Col_{h1} at 90 °C	35.3 (35.3)	(1 0)
	a = 40.6	20.0 (20.5)	(1 1)
	h = 4.1	17.7 (17.7)	(2 0)
		11.5 (11.8)	(3 0)
	n = 2.1[a]	8.2	halo
		ca. 4.6	broad
		ca. 4.1	"
	Col_{h2} at 130 °C	32.6 (32.6)	(1 0)
	a = 37.5	18.9 (18.8)	(1 1)
		16.1 (16.3)	(2 0)
	n = 2.1[b]	ca. 4.7	halo
[$L^{16}ZnCl_2$]	Col_h at 100 °C	37.0 (37.0)	(1 0)
	a = 42.7	21.5 (21.4)	(1 1)
		18.4 (18.5)	(2 0)
	n= 2.2[b]	17.5 (16.6)	(3 0)
		ca. 4.6	halo
[$L^{12}PdCl_2$]	Col_{h1} at 90 °C	35.0 (35.0)	(1 0)
	a = 40.3	20.1 (20.2)	(1 1)
	h = 3.8	17.4 (17.5)	(2 0)
		11.5 (11.8)	(3 0)
		8.0	halo
	n = 1.9[a]	ca. 4.6	"
		ca. 3.8	"
	Col_{h2} at 141 °C	32.7 (32.7)	(1 0)
	a = 38.0	18.8 (18.9)	(1 1)
		16.7 (16.4)	(2 0)
	n = 2.0[b]	7.3	halo
		ca. *4.8*	"
[$L^{16}PdCl_2$]	Col_h at 60 °C	43.6 (43.6)	(1 0)
		25.6 (25.2)	(1 1)
	a = 50.6	21.8 (21.8)	(2 0)
	h = 3.6	14.7 (14.5)	(3 0)
	n = 2.3[a]	ca. 4.6	halo
		ca. 3.6	"

[a] Number of molecules in each segment of the columns calculated with h = 4.1 and 3.6 Å. [b] Number of molecules in each segment of the columns calculated with h in the range 4.7−4.8 Å.

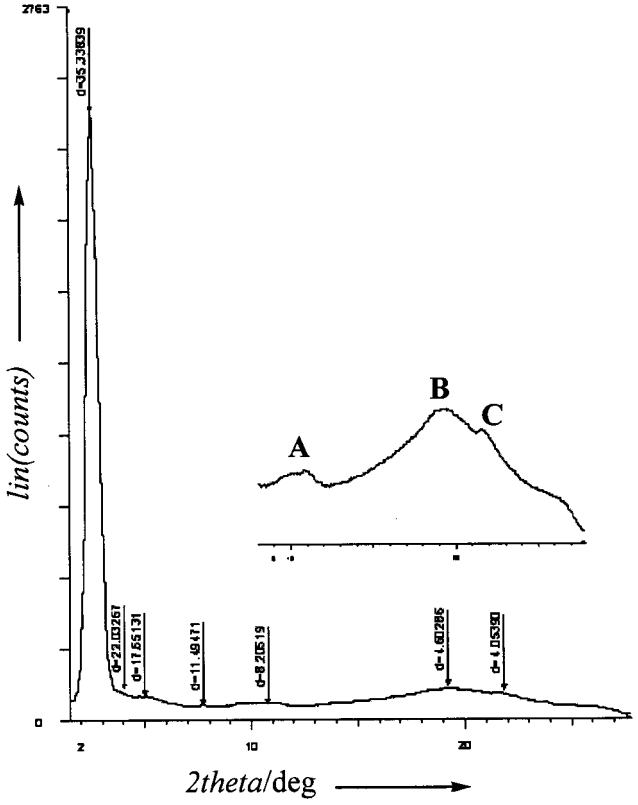

Figure 4. Powder X-ray diffraction pattern of the columnar hexagonal phase (Col_{h1}) at 90 °C for complex [$\mathbf{L^{12}ZnCl_2}$]

metry but a significant difference of the lattice parameter between [$\mathbf{L^{16}ZnCl_2}$] and [$\mathbf{L^{16}PdCl_2}$] was observed (Table 3). In fact, the noteworthy increase of *a* from 42.7 to 50.6 Å on going from the Zn^{II} to the Pd^{II} derivative is indicative of an increase of the size of the disk formed by the association of two molecules into a dimeric unit. At this particular length of the side chains, the geometry around the metal ion clearly plays an important role in the association of molecules into dimers. The flatness of the molecules in the case of the square planar Pd^{II} complex compared with the distorted tetrahedral Zn^{II} derivative encourages close proximity between the cores within the dimer (broad diffuse band in the XRD spectra at ca. 3.6 Å which corresponds to the distance between adjacent cores). In consequence, a larger horizontal displacement and an overall rise of the radius of the disk can be observed.

In both cases, a slight change of the position of the first peak in the low angle region was observed on increasing the temperature. A corresponding decrease in the intecolumnar distance to less than 1 Å was also observed. This slow change corresponds to a very low enthalpy (3.3 and 0.6 kJ/mol) and the absence of important optical textural changes.

Photoconductivity Measurements

Because of the incremental charge mobility induced by molecular self-assembling,[12] columnar mesophases have recently become attractive for their potential applications in organic photovoltaic and electroluminescent devices in which high conduction is required. In order to probe the effectiveness of our materials as photoconductors, we selected the longer chain length palladium and zinc derivatives and performed standard measurements as described in the Exp. Sect. Since pure samples show no absorption in the visible region, photogeneration was induced by doping with a small amount (0.05%) of C_{60} which is known as a good acceptor thereby promoting the formation of hole carriers. Phase transitions were not affected by the small amount of this dopant. Within our cells, it was not possible to obtain a homogeneous alignment of the mesophases using standard techniques and all the measurements were performed on unaligned samples. Figure 5 shows the ratio of the light and dark conductivities for [$\mathbf{L^{16}PdCl_2}$] at 633 nm over a temperature range which incorporates solid, columnar and isotropic phases.

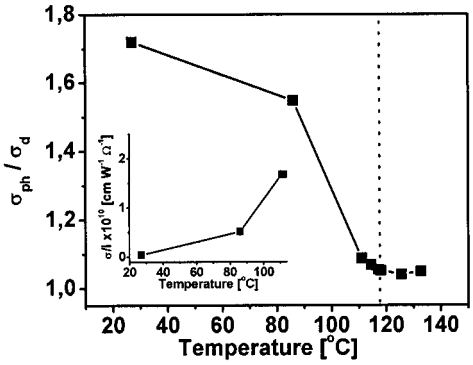

Figure 5. Ratio between the photoconductivity σ_{ph} and the conductivity in the dark σ_d for a 40 μm thick sample of complex [$\mathbf{L^{16}PdCl_2}$] doped with C_{60} as a function of temperature; the vertical line marks the I − Col_h transition; inset: normalised photoconduction measured as a function of temperature for the same sample; data were collected in an applied field of 8 V/μm and a wavelength λ = 633 nm

It is clearly visible that with decreasing temperature such a ratio starts to increase at the I-Col_h transition and keeps increasing upon further decreases in temperature. This is a signature of the reduced contribution of ionic (impurities) conduction at low temperatures compared with the contribution of electron (hole) hopping. The temperature dependence of the photoconductivity, normalised to the power density of the incident radiation, is shown in the inset of Figure 5, while its applied field dependence is shown in Figure 6. A proper comparison of conductivity with similar compounds would require mobility measurements which have not been yet carried out. Nevertheless, although the ratio of photo-conductivity to dark-conductivity is rather low, the measured values of the absolute photoconductivity are quite good, especially considering that the absorption coefficient for these samples at 633 nm is rather low ($\alpha \approx 16\ cm^{-1}$) and that for the relatively low values of the applied fields used, the photogeneration quantum efficiency should also be low.

The data in Figure 6 in fact show photoconductivity which is orders of magnitude higher than that measured for

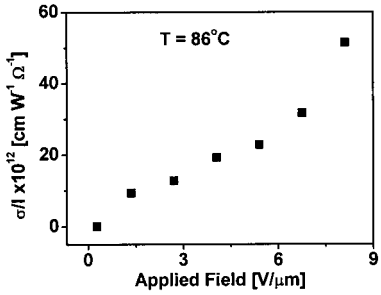

Figure 6. Normalised photoconduction at $\lambda = 633$ nm measured as a function of applied field for complex [$\mathbf{L^{16}PdCl_2}$] doped with C_{60}

standard photoconductors such as polyvinylcarbazole at the same applied field and with the same absorption coefficients. As a consequence, these results indicate that charge mobility in [$\mathbf{L^{16}PdCl_2}$] could be high and measurements are in progress to confirm this hypothesis. In the case of the related [$\mathbf{L^{16}ZnCl_2}$] complex, the measured photoconductivity is about two orders of magnitude lower. Since the measurements are in a preliminary stage, it is not possible at the moment to rationalise this behaviour.

Conclusions

A series of hexacatenar 4,4′-disubstituted 2,2′-bipyridines (**L″**) and the corresponding zinc(II) and palladium(II) complexes [$\mathbf{L''MCl_2}$] have been synthesised and characterised. Although the ligands are not mesomorphic, the association of the hemi-disc shaped molecules in face-to-face disc-shaped dimers induces columnar mesogenic properties for all the metal derivatives, regardless of the nature of metal atom. In fact, liquid crystal properties were also induced for the first time on tetrahedrally coordinated zinc complexes while for the palladium derivatives [$\mathbf{L''PdCl_2}$], the lamellar mesophases observed in dialkyl 2,2′-bipyridine-4,4′-dicarboxylate compounds[8a] are replaced by hexagonal columnar mesomorphism. Hence, it can be suggested that for all the new [$\mathbf{L''MCl_2}$] complexes in which the organic parts of the molecules have been modified through the introduction of further aromatic rings, the driving force in producing a supramolecular columnar arrangement is the existence of intermolecular interactions (hydrogen bonds, C−H−π and π−π contacts) between the large flat aromatic cores rather than dipolar or metal-metal interactions. The analysis of the crystal packing in the solid state of the model compound [$\mathbf{LPdCl_2}$] has given excellent insight into the future arrangements of the mesophases of the corresponding long chain derivatives, at least as far as the polar fragments of the molecules are concerned. The presence of long alkoxy chains in the [$\mathbf{L''MCl_2}$] derivatives gives rise to mesomorphism without interfering with the promesogenic columnar arrangement of the aromatic cores of the molecules.

Moreover, the thermal behaviour in each series was found to be insensitive to the nature of the metal atom and slightly decreases in the order Zn < Pd. This can be correlated with the overall supramolecular organisation rather than with the segregation effects of the simple molecular units.

These results show that by a careful choice of molecular building blocks, it is possible to finely modulate the interactions which determine the organisation of single molecules (association into dimers) in supramolecular architectures, giving rise to the desired functionalised metallomesogenic materials. For this class of derivatives, our goal was the design of metal-containing columnar liquid crystals in which the pre-selected property for improvement was the charge carrier mobility for charge transport. Preliminary measurements of photoconductivity, in samples of [$\mathbf{L''MCl_2}$] complexes doped with C_{60} to increase absorption in the visible, have given excellent results and further experiments are in progress.

Experimental Section

Materials and Measurements: All reagents were purchased from the following and used as received: 4,4′-Dimethyl-2,2′-bipyridine, benzoic acid, 1-bromododecane, 1-bromohexadecane, zinc chloride, 4-pyrrolidinopyridine (PPY) from Aldrich, methyl 3,4,5-trihydroxybenzoate from Lancaster and *N*,*N*′-dicyclohexylcarbodiimide (DCC) from Fluka. The solvents were used as received from commercial sources without further purification and were dried using standard methods when required. *cis*-Bis(benzonitrile)dichloropalladium,[22] 4,4′-bis(hydroxymethyl)-2,2′-bipyridine[23] and 3,4,5-trialkoxybenzoic acids[24] were prepared with slight changes following the methods described in the literature. Infrared spectra were recorded with a Spectrum One FT-IR Perkin−Elmer spectrometer and ^{1}H NMR spectra with a Bruker WH-300 spectrometer in [D_6]DMSO, $CDCl_3$ or CD_3OD with TMS as an internal standard. Elemental analyses were performed with a Perkin−Elmer 2400 analyser. The textures of the mesophases were examined with a Zeiss Axioscope polarising microscope equipped with a Linkam CO 600 heating stage. The transition temperatures and enthalpies were measured on a Perkin−Elmer Pyris1 Differential Scanning Calorimeter with a heating and cooling rate of 10 °C/min. The apparatus was calibrated with indium. Two or more heating/cooling cycles were performed on each sample. Spectrofluorimetric grade dichloromethane (Acros Organics) was used for the photophysical investigations in solution at room temperature. Absorption spectra were recorded with a Perkin−Elmer Lambda 900 spectrophotometer. The experimental uncertainty of the band maximum for the absorption spectra was 2 nm. The ligands and the complexes are stable in CH_2Cl_2 as demonstrated by the constancy of their absorption spectra over a week. The powder X-ray diffraction patterns were obtained using a Bruker AXS General Area Detector Diffraction System (D8 Discover with GADDS) with Cu-K_α radiation. The highly sensitive area detector was placed at a distance of 10 cm from the sample and equipped with a CalCTec (Italy) heating stage. The samples were heated at a rate of 5.0 °C min^{-1} to the appropriate temperature. Measurements were performed by placing samples in Lindemann capillary tubes with an inner diameter of 0.05 mm. Samples for photoconductivity measurements were prepared by mixing the complex [$\mathbf{L^{16}MCl_2}$] and 0.05% C_{60} in toluene and then evaporating the solvent. The resultant material was then transferred between two ITO-covered conducting glass slides by using the effect of capillarity within the isotropic phase. The thickness was controlled with glass spacers. The conductivity was measured by monitoring the voltage drop across a resistor in

series with the sample cell. For temperature dependent measurements, a CalCTec (Italy) hot stage was used. For photoconductivity observations, an approximately 10^{-2} cm^2 sample was illuminated with 5 mW of light from a He-Ne laser at 633 nm.

X-ray Crystallographic Data Collection and Refinement of the [LPdCl$_2$] Structure: Orange crystals of [**LPdCl$_2$**] were formed at room temperature from a DMSO/ethanol mixture. Diffraction measurements were carried out at room temperature on a Siemens *R*3*m*/*V* automated four-circle diffractometer equipped with graphite-monochromated Mo-K_α radiation (λ = 0.71073 Å). The data were corrected for Lorentz, polarisation and X-ray absorption effects using the XABS2 program.[25] Details of the crystal data collection are listed in Table 4. Structure solution (Patterson method) and full-matrix least-squares refinements based on F^2 were performed with the SHELXS/L programs of the SHELXTL-NT software package (Version 5.10).[26] All nonhydrogen atoms were refined anisotropically. The hydrogen atoms were included in the refinement in their observed positions and then fixed as idealised atoms riding on the respective carbon atom. CCDC-241996 contains the supplementary crystallographic data for this paper. These data can be obtained free of charge at www.ccdc.cam.ac.uk/conts/retrieving.html or from the Cambridge Crystallographic Data Centre, 12 Union Road, Cambridge CB2 1EZ, UK; Fax: (internat.) + 44-1223-336-033; E-mail: deposit@ccdc.cam.ac.uk].

Table 4. Crystal and structure refinements for complex [**LPdCl$_2$**]

Formula	$C_{26}H_{20}Cl_2N_2O_4Pd$
M_r	601.7
Crystal system	triclinic
Space group	$P\bar{1}$
a (Å)	9.671(2)
b (Å)	11.329(3)
c (Å)	11.484(3)
α (°)	99.06(2)
β (°)	95.20(2)
γ (°)	105.48(2)
V (Å^3)	1185.7(4)
T (K)	298
Z	2
Density (Mg/m^{-3})	1.685
Absorption coefficient (mm^{-1})	1.045
F(000)	604
Reflections collected	4483
Unique reflections [$I > 2\sigma(I)$]	4213 (2447)
R(int)	0.037
Parameters	314
R_1[a] [$I > 2\sigma(I)$]	0.0486
wR_2[b] (all data)	0.1006
GOF on F^2	0.825

[a] $R1 = \Sigma(|F_o| - |F_c|)/\Sigma|F_o|$. [b] $wR2 = \{\Sigma[w(F_o^2 - F_c^2)^2]/\Sigma[w(F_o^2)^2]\}^{1/2}$.

Synthesis

Model Ligand: 4,4′-Bis(benzoyloxymethyl)-2,2′-bipyridine (L): 4,4′-Bis(hydroxymethyl)-2,2′-bipyridine (0.099 mg, 0.46 mmol), benzoic acid (0.112 g, 0.92 mmol) and DCC (0.208 g, 1.01 mmol) were suspended in dry dichloromethane (20 mL). PPY (0.013 g, 0.09 mmol) was added and the reaction was stirred at room temperature and under N_2 for a week. The colourless precipitate was removed by filtration and the solvent was evaporated. The crude product was recrystallised from chloroform/methanol giving a colourless solid. Yield 0.161 g (82%); m.p. 179 °C. ^{1}H NMR (300 MHz, $CDCl_3$, 25 °C, TMS): δ = 5.47 (s, 4 H, CH_2), 7.49 (m, 2 H, CH), 7.58 (m, 4 H, CH), 7.61 (m, 4 H, CH), 8.13 (dd, $^3J_{H,H}$ = 8.5, $^4J_{H,H}$ = 2.4 Hz, 2 H, H-5 bpy), 8.48 (s, 2 H, H-3 bpy), 8.70 (d, $^3J_{H,H}$ = 8.5 Hz, 2 H, H-6 bpy) ppm. IR (KBr): $\tilde{\nu}$ = 1723 cm^{-1} (C=O). UV/Vis (dichloromethane): $\lambda_{max.}$ (ε, mol^{-1}·dm^3·cm^{-1}) = 282 nm (17800). $C_{26}H_{20}N_2O_4$ (424.46): calcd. C 73.57, H 4.57, N 6.60; found C 73.44, H 4.62, N 6.76. All **L^n** ligands were prepared similarly starting from 4,4′-bis(hydroxymethyl)-2,2′-bipyridine and the appropriate 3,4,5-trialkoxy-substituted benzoic acid. Therefore only yields, melting points, ^{1}H NMR data, IR data and elemental analyses are reported below.

4,4′-Bis[3,4,5-(tridodecyloxy)benzoyloxymethyl]-2,2′-bipyridine (L^{12}): Yield 0.62 g (78%); m.p. 73 °C. ^{1}H NMR (300 MHz, $CDCl_3$, 25 °C, TMS): δ = 0.88 (t, $^3J_{H,H}$ = 6.6 Hz, 18 H, CH_3), 1.26 [m, 108 H, $(CH_2)_5CH_3$], 1.78 [m, 12 H, $CH_2(CH_2)_5CH_3$], 4.03 (t, $^3J_{H,H}$ = 6.3 Hz, 12 H, OCH_2), 5.44 (s, 4 H, CH_2), 7.33 (s, 4 H, CH), 7.37 (d, $^3J_{H,H}$ = 4.7 Hz, 2 H, H-5 bpy), 8.49 (s, 2 H, H-3 bpy), 8.67 (d, $^3J_{H,H}$ = 4.7 Hz 2 H, H-6 bpy) ppm. IR (KBr): $\tilde{\nu}$ = 1720 cm^{-1} (C=O). UV/Vis (dichloromethane): $\lambda_{max.}$ (ε, mol^{-1}·dm^3·cm^{-1}) = 277 nm (39100). $C_{98}H_{164}N_2O_{10}$ (1530.39): calcd. C 76.91, H 10.80, N 1.83; found C 76.72, H 11.00, N 2.01.

4,4′-Bis[3,4,5-(trihexadecyloxy)benzoyloxymethyl]-2,2′-bipyridine (L^{16}): Yield 0.35 g (63%); m.p. 90 °C. ^{1}H NMR (300 MHz, $CDCl_3$, 25 °C, TMS): δ = (t, $^3J_{H,H}$ = 6.6 Hz, 18 H, CH_3), 1.25 [m, 156 H, $(CH_2)_5CH_3$], 1.77 [m, 12 H, $CH_2(CH_2)_5CH_3$], 4.02 (m, 12 H, OCH_2), 5.44 (s, 4 H, CH_2), 7.33 (s, 4 H, CH), 7.37 (d, $^3J_{H,H}$ = 5.0 Hz, 2 H, H-5 bpy), 8.49 (s, 2 H, H-3 bpy), 8.68 (d, $^3J_{H,H}$ = 5.0 Hz, 2 H, H-6 bpy) ppm. IR (KBr): $\tilde{\nu}$ = 1704 cm^{-1} (C=O). UV/Vis (dichloromethane): $\lambda_{max.}$ (ε, mol^{-1}·dm^3·cm^{-1}) = 278 nm (88700). $C_{122}H_{212}N_2O_{10}$ (1867.02): calcd. C 78.48, H 11.44, N 1.50; found C 78.55, H 11.50, N 1.70.

Zinc Complexes: All zinc complexes were prepared in a similar manner. The synthesis of [**LZnCl$_2$**] is described in detail below and for all other homologues only yields, ^{1}H NMR and IR data and elemental analyses are reported.

[4,4′-Bis(benzoyloxymethyl) 2,2′-bipyridyl]zinc(II) Chloride [LZnCl$_2$]: A suspension of $ZnCl_2$ (0.013 g, 0.094 mmol) and **L** (0.040 g, 0.094 mmol) in dichloromethane (10 mL) was stirred at room temperature for four days. By filtration through Celite and evaporation the final product was obtained as a colourless solid after recrystallisation from methanol. Yield 0.37 g (70%); m.p. 260 °C. ^{1}H NMR (300 MHz, CD_3OD, 25 °C, TMS): δ = 5.61 (s, 4 H, CH_2), 7.51 (m, 4 H, CH), 7.65 (m, 2 H, CH), 7.83 (m, 4 H, CH), 8.12 (d, $^3J_{H,H}$ = 7.3 Hz, 2 H, H-5 bpy), 8.75−8.68 (m, 4 H, H-3,6 bpy) ppm. IR (KBr): $\tilde{\nu}$ = 1720 cm^{-1} (C=O). $C_{26}H_{20}Cl_2N_2O_4Zn$ (560.74): calcd. C 55.69, H 3.60, N 5.00; found C 55.48, H 3.58, N 4.74.

{4,4′-Bis[3,4,5-tridodecyloxy)benzoyloxymethyl]-2,2′-bipyridyl}-zinc(II) Chloride [L^{12}ZnCl$_2$]: Recrystallisation from dichloromethane/diethyl ether. Yield 0.160 g (86%); thermotropic behaviour in Table 2. ^{1}H NMR (300 MHz, $CDCl_3$, 25 °C, TMS): δ = 0.88 (t, $^3J_{H,H}$ = 6.4 Hz, 18 H, CH_3), 1.26 [m, 108 H, $(CH_2)_5CH_3$], 1.79 [m, 12 H, $CH_2(CH_2)_5CH_3$], 4.03 (m, 12 H, OCH_2), 5.52 (s, 4 H, CH_2), 7.29 (s, 4 H, CH), 7.78 (d, $^3J_{H,H}$ = 5.3 Hz, 2 H, H-5 bpy), 8.24 (s, 2 H, H-3 bpy), 8.85 (d, $^3J_{H,H}$ = 5.3 Hz, 2 H, H-6 bpy) ppm. IR (KBr): $\tilde{\nu}$ = 1718 cm^{-1} (C=O). UV/Vis (dichloromethane): $\lambda_{max.}$ (ε, mol^{-1}·dm^3·cm^{-1}) = 282 (30500), 297 (31400), 307 nm (27700). $C_{98}H_{164}Cl_2N_2O_{10}Zn$ (1666.67): calcd. C 70.62, H 9.92, N 1.68; found C 70.31, H 9.63, N 1.90.

{4,4′-Bis(3,4,5-tris[hexadecyloxy)benzoyloxymethyl]-2,2′-bipyridyl}-zinc(II) Chloride [$L^{16}ZnCl_2$]: Recrystallisation by chloroform/acetone. Yield 0.12 g (91%); thermotropic behaviour in Table 2. ^{1}H NMR (300 MHz, $CDCl_3$, 25 °C, TMS): δ = 0.87 (t, $^3J_{H,H}$ = 6.7 Hz, 18 H, CH_3), 1.25 [m, 156 H, $(CH_2)_5CH_3$], 1.80 [m, 12 H, $CH_2(CH_2)_5CH_3$], 4.03 (m, 12 H, OCH_2), 5.52 (s, 4 H, CH_2), 7.28 (s, 4 H, CH), 7.77 (d, $^3J_{H,H}$ = 5.1 Hz, 2 H, H-5 bpy), 8.24 (s, 2 H, H-3 bpy), 8.86 (d, $^3J_{H,H}$ = 5.1 Hz, 2 H, H-6 bpy) ppm. IR (KBr): $\tilde{\nu}$ = 1720 cm^{-1} (C=O). UV/Vis (dichloromethane): $\lambda_{max.}$ (ε, $mol^{-1}\cdot dm^3\cdot cm^{-1}$) = 282 (25600), 296 (27400), 307 nm (24600). $C_{122}H_{212}Cl_2N_2O_{10}Zn$ (2003.32): calcd. C 73.15, H 10.67, N 1.40; found C 73.38, H 10.90, N 1.48.

Palladium Complexes: All palladium complexes were prepared in a similar manner. The synthesis of **[$LPdCl_2$]** is described in detail below. For all other homologues only yields, ^{1}H NMR and IR data and elemental analyses are reported.

[4,4′-Bis(benzoyloxymethyl)-2,2′-bipyridyl]palladium(II) Chloride [$LPdCl_2$]: A solution of $[Pd(PhCN)_2Cl_2]$ (0.045 g, 0.12 mmol) and **L** (0.20 g, 0.17 mmol) in chloroform (10 mL) was heated to reflux for 7 h. Filtration and washing with methanol gave the final product as a pale yellow solid. Yield 0.08 g (80%); m.p. 322 °C. ^{1}H NMR (300 MHz, [D$_6$]DMSO, 25 °C, TMS): δ = 5.59 (s, 4 H, CH_2), 7.56 (m, 4 H, CH), 7.70 (m, 2 H, CH), 7.90 (d, 4 H, CH), 8.105 (dd, $^3J_{H,H}$ = 6.85, $^4J_{H,H}$ = 1.4 Hz, 2 H, H-5 bpy), 8.68 (s, 2 H, H-3 bpy), 9.075 (d, $^3J_{H,H}$ = 6.85 Hz, 2 H, H-6 bpy) ppm. IR (KBr): $\tilde{\nu}$ = 1720 cm^{-1} (C=O). $C_{26}H_{20}Cl_2N_2O_4Pd$ (601.78): calcd. C 51.89, H 3.35, N 4.66; found C 51.63, H 3.35, N 4.62.

{4,4′-Bis[3,4,5-tri(dodecyloxy)benzoyloxymethyl]-2,2′-bipyridyl}-palladium(II) Chloride [$L^{12}PdCl_2$]: Recrystallisation from chloroform/methanol. Yield 0.21 g (93%); thermotropic behaviour in Table 2. ^{1}H NMR (300 MHz, $CDCl_3$, 25 °C, TMS): δ = 0.87 (m, 18 H, CH_3), 1.26 (m, 108 H, $(CH_2)_5CH_3$], 1.78 (m, 12 H, $CH_2(CH_2)_5CH_3$], 4.02 (m, 12 H, OCH_2), 5.52 (s, 4 H, CH_2), 7.29 (s, 4 H, CH), 7.48 (d, $^3J_{H,H}$ = 5.2 Hz, 2 H, H-5 bpy), 8.18 (s, 2 H, H-3 bpy), 9.10 (d, $^3J_{H,H}$ = 5.2 Hz, 2 H, H-6 bpy) ppm. IR (KBr): $\tilde{\nu}$ = 1723 cm^{-1} (C=O). UV/Vis (dichloromethane): $\lambda_{max.}$ (ε, $mol^{-1}\cdot dm^3\cdot cm^{-1}$) = 268 (36600), 304 (24700) 314 nm (23000). $C_{98}H_{164}Cl_2N_2O_{10}Pd$ (1707.71): calcd. C 68.93, H 9.68, N 1.64; found C 69.15, H 9.50, N 1.37.

{4,4′-Bis[3,4,5-tri(hexadecyloxy)benzoyloxymethyl]-2,2′-bipyridyl}-palladium(II) Chloride [$L^{16}PdCl_2$]: Yield 0.20 g (91%); thermotropic behaviour in Table 2. ^{1}H NMR (300 MHz, $CDCl_3$, 25 °C, TMS): δ = 0.87 (t, $^3J_{H,H}$ = 6.5 Hz, 18 H, CH_3), 1.25 [m, 156 H, $(CH_2)_5CH_3$], 1.78 [m, 12 H, $CH_2(CH_2)_5CH_3$], 4.02 (m, 12 H, OCH_2), 5.52 (s, 4 H, CH_2), 7.29 (s, 4 H, CH), 7.49 (d, $^3J_{H,H}$ = 5.8 Hz, 2 H, H-5 bpy), 8.16 (s, 2 H, H-3 bpy), 9.11 (d, $^3J_{H,H}$ = 5.8 Hz, 2 H, H-6 bpy) ppm. IR (KBr): $\tilde{\nu}$ = 1721 cm^{-1} (C=O). UV/Vis (dichloromethane): $\lambda_{max.}$ (ε, $mol^{-1}\cdot dm^3\cdot cm^{-1}$) = 268 (43900), 304 (26400), 314 nm (22800). $C_{122}H_{212}Cl_2N_2O_{10}Pd$ (2044.35): calcd. C 71.68, H 10.45, N 1.37; found C 71.83, H 10.22, N 1.65.

Acknowledgments

This work was partly supported by CIPE grants (Clusters 14 and 26) from the Ministero dell'Istruzione, dell'Università e della Ricerca. P. P. is pleased to acknowledge the Marie Curie development host fellowship Contract HPMD-CT-2001-00073 for financial support.

[1] J. L. Serrano, *Metallomesogens*, Wiley-VCH, Weinheim, **1996**.
[2] B. Donnio, D. W. Bruce, in *Structure and Bonding* (Ed.: D. M. P. Mingos), Springer, Berlin, **1999**, vol. 95.
[3] R. W. Date, E. F. Iglesias, K. E. Rowe, J. M. Elliott, D. W. Bruce, *Dalton Trans.* **2003**, 1914−1932.
[4] R. Giménez, D. P. Lydon, J. L. Serrano, *Curr. Opin. Sol. State Mat. Sci.* **2002**, *6*, 527−535.
[5] [5a] I. Aiello, M. Ghedini, M. La Deda, D. Pucci, O. Francescangeli, *Eur. J. Inorg. Chem.* **1999**, 1367−1372. [5b] C. Tschierske, *Angew. Chem. Int. Ed.* **2000**, *39*, 2454−2458. [5c] H. Richtzenhain, A. J. Blake, D. W. Bruce, I. A. Fallis, W-S. Li, M. Schröder, *Chem. Commun.* **2001**, 2580−2581. [5d] M. Benouazzane, S. Coco, P. Espinet, J.-M. Martin-Alvarez, J. Barbera, *J. Mater. Chem.* **2002**, *12*, 691−696. [5e] L. Plasseraud, L. Gonzales Cuervo, D. Guillon, G. Suss-Fink, R. Deschenaux, D. W. Bruce, B. Donnio, *J. Mater. Chem.* **2002**, *12*, 2653−2658. [5f] D. M. Huck, H. Loc Nguyen, H. Coles, M. Hursthouse, B. Donnio, D. W. Bruce, *J. Mater. Chem.* **2002**, *12*, 2879−2886. [5g] L. Douce, T.-H. Diep, R. Ziessel, A. Skoulios, M. Césario, *J. Mater. Chem.* **2003**, *13*, 1533−1539.
[6] J. L. Serrano, T. Sierra, *Chem. Eur. J.* **2000**, *6*, 759−766.
[7] T. Kato, N. Mizoshita, *Curr. Opin. Sol. State Mat. Sci.* **2002**, *6*, 579−587.
[8] [8a] D. Pucci, G. Barberio, A. Crispini, O. Francescangeli, M. Ghedini, *Mol. Cryst. Liq. Cryst.* **2003**, *395*, 325−335. [8b] D. Pucci, G. Barberio, A. Crispini, O. Francescangeli, M. Ghedini, M. La Deda, *Eur. J. Inorg. Chem.* **2003**, *19*, 3649−3661.
[9] A. G. Serrette, T. M. Swager, *J. Am. Chem. Soc.* **1993**, *115*, 8879−8880.
[10] J. Bushby, O. R. Lozman, *Curr. Opin. Coll. Interf. Sci.* **2002**, *7*, 343−354.
[11] R. J. Busby, O. R. Lozman, *Curr. Opin. Sol. State Mat. Sci.* **2002**, *6*, 569−578.
[12] M. O'Neill, S. M. Kelly, *Adv. Mater.* **2003**, *15*, 1135−1146.
[13] F. Morale, R. W. Date, D. Guillon, D. W. Bruce, R. L. Finn, C. Wilson, A. J. Blake, M. Schroder, B. Donnio, *Chem. Eur. J.* **2003**, *9*, 2484−2501.
[14] A. Pegenau, T. Hegmann, C. Tschierske, S. Diele, *Chem. Eur. J.* **1999**, *5*, 1643−1660.
[15] E. Terazzi, J.-M. Bénech, J.-P. Rivera, G. Bernardinelli, B. Donnio, D. Guillon, C. Piguet, *Dalton Trans.* **2003**, 769−772.
[16] A. N. Cammidge; H. Gopee, *Chem. Commun.* **2002**, 966−967.
[17] G. R. Desiraju, T. Steiner, in *The Weak Hydrogen Bond* (IUCr Monograph on Crystallography 9), Oxford Science Publ., **1999**.
[18] C. Janiak, *J. Chem. Soc., Dalton Trans.* **2000**, 3885−3896.
[19] A.-J. Attias, C. Cavalli, B. Donnio, D. Guillon, P. Hapiot, J. Malthête, *Chem. Mater.* **2002**, *14*, 375−384.
[20] [20a] S. T. Trzaska, T. M. Swager, *Chem. Mater.* **1998**, *10*, 438−443. [20b] T. Hegmann, J. Kain, S. Diele, B. Schubert, H. Bögel, C. Tschierske, *J. Mater. Chem.* **2003**, *13*, 991−1003.
[21] H. Zheng, C. K. Lai, T. M. Swager, *Chem. Mater.* **1995**, *7*, 2067−2077.
[22] M. S. Karash, R. C. Seyler, F. R. Mayo, *J. Am. Chem. Soc.* **1938**, *60*, 882−885.
[23] G. Will, G. Boschloo, S. Nagaraja Rao, D. Fitzmaurice, *J. Phys. Chem. B* **1999**, *103*, 8067−8079.
[24] K.E. Rowe, D.W. Bruce, *J. Mater. Chem.* **1998**, *8*, 331−341.
[25] S. Parkin, B. Moezzi, H. J. Hope, *Appl. Crystallogr.* **1995**, *28*, 53−56.
[26] *SHELXTL/NT* crystal structure analysis package, Bruker AXS, Inc.: Madison, WI, **1999**.

Received June 17, 2004
Early View Article
Published Online November 10, 2004

